Synthesis and Optoelectronic Properties of Novel Benzodifuran Semiconducting Polymers

Prakash Sista, Peishen Huang, Samodha S. Gunathilake, Mahesh P. Bhatt, Ruvini S. Kularatne, Mihaela C. Stefan, Michael C. Biewer

Department of Chemistry, University of Texas at Dallas, Richardson, Texas 75080
Correspondence to: M. C. Biewer (E-mail: biewerm@utdallas.edu)

Received 21 May 2012; accepted 25 June 2012; published online 20 July 2012
DOI: 10.1002/pola.26243

ABSTRACT: Two new semiconducting polymers poly{4,8-bis(4-decylphenylethynyl)benzo[1,2-*b*:4,5-*b*′]difuran} (**P1**) and poly {4,8-bis(4-decylphenylethynyl)benzo[1,2-*b*:4,5-*b*′]difuran-*alt*-4,8-bis(4-decylphenylethynyl)benzo[1,2-*b*:4,5-*b*′]dithiophene} (**P2**) have been synthesized. These polymers were tested in bulk heterojunction solar cells yielding power conversion efficiencies of 1.19% for **P1** and 0.79% for **P2**. The surface morphology of the solar cell devices indicated that both the polymers display a granular morphology with smoother films displaying higher power conversion efficiencies. © 2012 Wiley Periodicals, Inc. J Polym Sci Part A: Polym Chem 50: 4316–4324, 2012

KEYWORDS: atomic force microscopy (AFM); conjugated polymers; UV-vis spectroscopy

INTRODUCTION Thiophene semiconducting polymers have been in the forefront of organic electronics research in the last decade.[1,2] Poly(3-hexylthiophene) (P3HT) is one of the most used semiconducting polymers in organic electronics applications,[2–4] and P3HT has predominantly found applications in organic solar cells[3,4] and field-effect transistors.[5] However, because of the position of the highest occupied molecular orbital (HOMO) energy level of P3HT relative to the lowest unoccupied molecular orbital (LUMO) of the acceptor [6,6]-phenyl-C_{61}-butyric acid methyl ester (PCBM), the open-circuit voltage obtained in bulk heterojunction solar cells with P3HT donor is relatively low.[2] To enhance the light absorption and to fine tune the energy levels of the polymers, a variety of fused-ring building blocks have been used.[6–20] Benzo[1,2-*b*:4,5-*b*′]dithiophene (BDT) has gained significant interest among the fused-ring thiophenes because of its symmetrical structure and the ability to incorporate substituents on the central benzene core.[7–10,15–18,21]

BDT-based polymers have demonstrated good performance in both bulk heterojunction solar cells[17] and field-effect transistors.[9,13,14,18,22–24] Currently, a power conversion efficiency (PCE) of 8.37% has been reported by Cao and coworkers[25] using BDT-based polymers as electron donors in bulk heterojunction solar cells. Moreover, field-effect mobility as high as 0.15–0.25 $cm^2\ V^{-1}\ s^{-1}$ have been reported for BDT semiconducting polymers.[14] Replacing the thiophene with furan moieties could potentially lead to favorable changes in the optoelectronic properties of the polymers. When compared with thiophene semiconducting polymers, the furan polymers showed enhanced solubility.[26] Although the mechanism behind improved solubility is not well established, it may be due to the differences in atomic radius, electronegativity, and polarizability of oxygen versus sulfur atoms, which may impact solvent and intermolecular interactions.[26] Furthermore, furan can be manufactured from renewable, plant-derived sources enabling the synthesis of biorenewable materials.[27]

Benzo[1,2-*b*:4,5-*b*′]difuran (BDF) building block possesses unique properties[28] because furan displays weaker steric hindrance to adjacent units due to the smaller oxygen atom when compared with sulfur.[29] Consequently, polymerization of benzodifuran is expected to yield a more planar polymer backbone with increased conjugation length. Thus, BDF semiconducting polymers with smaller bandgap and improved optoelectronic properties could be envisioned. For example, Decurtins and coworkers[30] reported the synthesis of BDF semiconducting polymers and their use in bulk heterojunction solar cells. The PCEs reported initially for BDF polymers was only 0.17–0.59%.[30] However, recently, a PCE of ~5% was reported for a donor–acceptor copolymer of BDF.[28]

In this article, we report the synthesis and optoelectronic properties of two benzodifuran polymers containing decylphenylethynyl substituents. This work is an extension of our previous work on semiconducting polymers of benzodithiophene with decyl phenylethynyl substituents.[18] Synthesis, characterization, and photovoltaic performance of a

Additional Supporting Information may be found in the online version of this article.

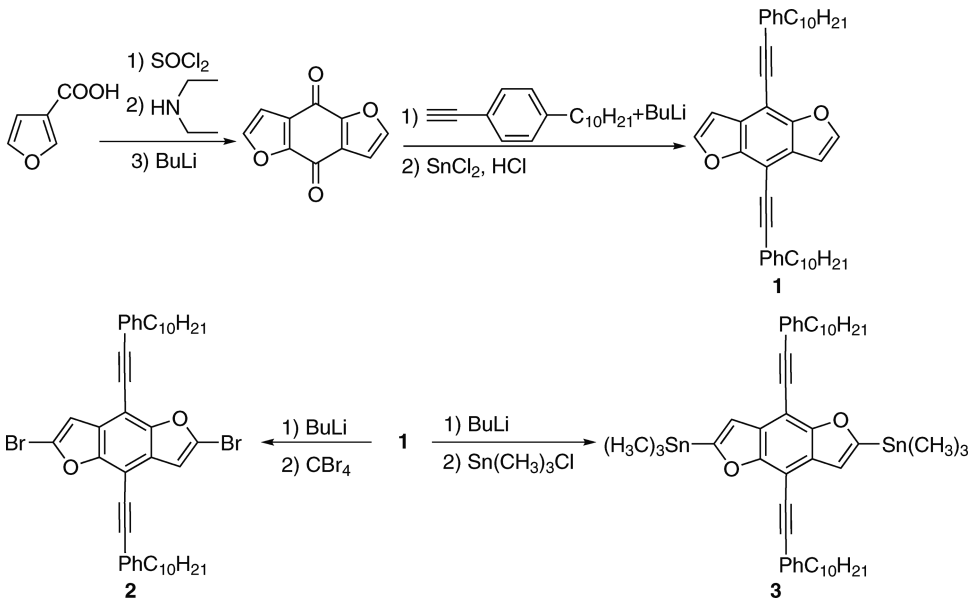

SCHEME 1 Synthesis of benzodifuran monomers.

homopolymer of BDF with decyl phenylethynyl substituents and an alternating copolymer of BDF and BDT with decyl phenylethynyl substituents are reported.

RESULTS AND DISCUSSION

4,8-Bis(4-decylphenylethynyl)benzo[1,2-*b*:4,5-*b*′]difuran has been synthesized similar to a procedure described in our earlier publication (Scheme 1).[18] Furan-3-carboxylic acid was reacted with thionyl chloride to obtain the acid chloride, which was further reacted with diethyl amine to generate *N, N*-diethyl furan-3-carboxamide. The amide was reacted with *n*-BuLi to form 4,8-dihydrobenzo[1,2-*b*:4,5-*b*′]difuran-4,8-dione. Precursor 4-decyl-1-ethynylbenzene was synthesized according to our published procedure.[18] The acetylide anion of 4-decyl-1-ethynylbenzene was reacted with 4,8-dihydrobenzo[1,2-*b*:4,5-*b*′]difuran-4,8-dione to generate 4,8-bis(4-decylphenylethynyl)benzo[1,2-*b*:4,5-*b*′]difuran (**1**) monomer after subsequent aromatization with $SnCl_2$ (Scheme 1). Lithiated monomer (**1**) was reacted with trimethyltin chloride and carbon tetrabromide to generate the distannylated and dibromo derivatives, respectively, which were used in Stille coupling polymerization to obtain poly{4,8-bis(4-decylphenylethynyl)benzo[1,2-*b*:4,5-*b*′]difuran} (**P1**) homopolymer (Fig. 1).

Stille coupling polymerization of 2,6-dibromo-4,8-bis(4-decylphenylethynyl)benzo[1,2-*b*:4,5-*b*′]difuran and 2,6-(trimethyltin)-4,8-bis(4-decylphenylethynyl)benzo[1,2-*b*:4,5-*b*′]dithiophene yielded the alternating copolymer poly{4,8-bis(4-decylphenylethynyl)benzo[1,2-*b*:4,5-*b*′]difuran-*alt*-4,8-bis(4-decyl-

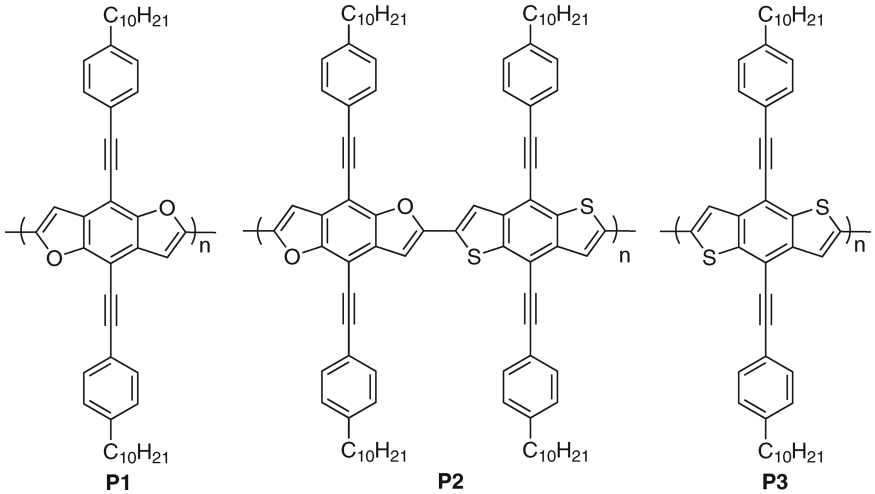

FIGURE 1 Structures of benzodifuran and benzodithiophene polymers: poly{4,8-bis(4-decylphenylethynyl)benzo[1,2-*b*:4,5-*b*′]difuran} (**P1**), poly{4,8-bis(4-decylphenylethynyl)benzo[1,2-*b*:4,5-*b*′]difuran-*alt*-4,8-bis(4-decylphenylethynyl)benzo[1,2-*b*:4,5-*b*′]dithiophene} (**P2**), and poly{4,8-bis(4-decylphenylethynyl)benzo[1,2-*b*:4,5-*b*′]dithiophene} (**P3**).

TABLE 1 Molecular Weights and Optoelectronic Properties of the Synthesized Polymers

Polymer	M_n[a] (g mol^{-1})	PDI[a]	λ_{max} ($CHCl_3$)[b] (nm)	λ_{max} (Film)[c] (nm)	HOMO[d] (eV)	LUMO[e] (eV)	E_g (eV)
P1	29,600	2.2	326, 522	333, 531	−5.39	−3.32	2.07
P2	22,500	2.5	350, 524	357, 541	−5.30	−3.26	2.04
P3	23,400	3.0	363, 520	366, 525	−5.10	−3.05	2.05

[a] Estimated from SEC.
[b] UV–vis absorption maxima of polymer solution in chloroform.
[c] UV–vis absorption maxima of polymer film drop-cast from chloroform solution.
[d] Estimated from the onset oxidation peak from a cyclic voltammogram.
[e] Estimated from the onset of reduction peak of the cyclic voltammogram.

phenylethynyl)benzo[1,2-*b*:4,5-*b*′] dithiophene} (**P2**) (Fig. 1). The structure of the benzodithiophene polymer (**P3**) analog is also shown in Figure 1 for comparison.

The polymers **P1** and **P2** were soluble in organic solvents like THF and $CHCl_3$. However, it was observed that the solubility of both the polymers in $CHCl_3$ was slightly lower than that of homopolymer poly{4,8-bis(4-decylphenylethynyl)-benzo[1,2-*b*:4,5-*b*′]dithiophene} (**P3**) already published by our group.[18] The number–average molecular weights of both **P1** (29,600 g mol^{-1}) and **P2** (22,500 g mol^{-1}) were comparable with that reported for benzodithiophene homopolymer **P3** (Table 1). UV–visible absorption spectra of both the polymers **P1** and **P2** were recorded in chloroform solution as well as in thin films (Fig. 2 and Table 1). Both spectra displayed two absorption maxima at ∼340 nm and ∼530 nm. The peak at ∼340 nm arises from the conjugation along the 1,4-bis(phenylethynyl)benzene side chains, whereas the peak at ∼530 nm originates from the π–π^* transition of the benzodifuran backbone.[18,31,32] A vibronic peak was observed at 558 nm in $CHCl_3$ and at 569 nm in film in the UV–vis spectra of **P1**. In contrast, the absorption peak arising from the backbone of **P2** was broader and did not display a vibronic peak. Red shift of both 1,4-bis(phenylethynyl)benzene absorption and benzodifuran backbone absorption peaks can be observed in the solid-state UV–vis spectra (Supporting Information). The absorption maxima of **P1** shifted from 327 nm (in $CHCl_3$) to 331 nm (in film) and from 524 nm (in $CHCl_3$) to 533 nm (in film). The absorption maxima of **P2** shifted from 348 nm (in $CHCl_3$) to 356 nm (in film) and from 524 nm (in $CHCl_3$) to 541 nm (in film). The relatively small red shift of the absorption bands in film combined with the vibronic peaks indicates the presence of rigid rod conformation in both the solution and solid states of **P1** and **P2**.[20,33]

The HOMO and LUMO energy levels of **P1** and **P2** were calculated from the values of onset of oxidation wave and onset of reduction wave measured using cyclic voltammetry (Table 1 and Supporting Information). The polymers exhibit HOMO energy levels of −5.39 eV for **P1** and −5.30 for **P2**. The more electronegative oxygen atom and the less polarizable carbon–oxygen bond make the furan unit a weaker donor, and hence, a deeper HOMO energy level was measured for **P1** when compared with the benzodithiophene homopolymer **P3** (Table 1).[34] The HOMO energy levels of both these polymers are lower than the air oxidation threshold indicating good air stability. Similarly, the LUMO energy levels of both the polymers are close to each other, −3.32 eV for **P1** and −3.26 eV for **P2**. The closeness of the HOMO and LUMO energy levels of **P1** and **P2** is due to the similarity in their structures and their molecular weights. The energy bandgaps of both **P1** and **P2** are similar to **P3**.[34]

Bulk heterojunction solar cells were fabricated using both polymers **P1** and **P2** with PCBM as the acceptor. A

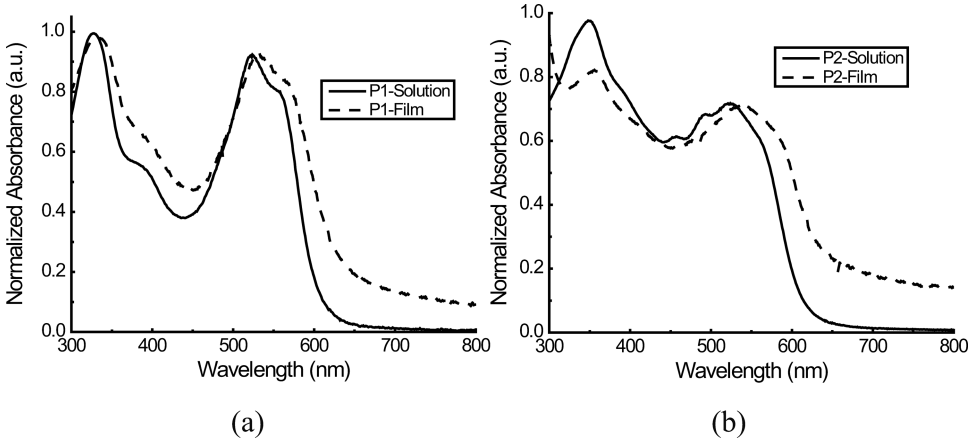

FIGURE 2 Solution and film UV–vis absorption spectra of polymers: (a) poly{4,8-bis(4-decylphenylethynyl)benzo[1,2-*b*:4,5-*b*′]difuran} (**P1**); (b) poly{4,8-bis(4-decylphenylethynyl)benzo[1,2-*b*:4,5-*b*′]difuran-*alt*-4,8-bis(4-decylphenylethynyl)benzo[1,2-*b*:4,5-*b*′]dithiophene} (**P2**); dotted line: film; solid line: solution (chloroform solvent).

TABLE 2 Bulk Heterojunction Solar Cell Data for Polymers **P1** and **P2**

Polymer	[P]:[PCBM]	V_{oc} (V)	J_{SC} (mA cm^{-2})	FF	η (%)	Film Thickness (nm)
P1	1:1	0.83	3.71	0.39	1.19	70.1
P1	1:2	0.82	3.34	0.39	1.06	73.6
P2	1:1	0.81	2.13	0.37	0.64	70.5
P2	1:2	0.81	2.24	0.44	0.79	67.0

conventional solar cell device structure of indium tin oxide (ITO)/poly(3,4-ethylenedioxythiophene):poly(styrenesulfonate) (PEDOT:PSS)/polymer:PCBM/Ca/Al was used for the measurements. The devices were optimized at 15 mg mL^{-1} concentration of the polymer/PCBM blend in chloroform solvent and at polymer:PCBM weight ratios of 1:1 and 1:2 (Table 2). The highest PCE for polymer **P1** (1.19%) was obtained for a device with 1:1 weight ratio of polymer and PCBM. Polymer **P1** displayed a relatively high V_{oc} of ~0.82 V for both 1:1 and 1:2 devices. Polymer **P2** displayed the highest PCE of 0.79% at 1:2 weight ratio. The measured V_{oc} of **P2** was about 0.81 V. The higher V_{oc} measured for polymers **P1** and **P2** are due to their deeper HOMO energy levels when compared with polymer **P3**. The measured V_{oc} for polymers **P1** and **P2** are in close agreement with the theoretical calculated values.[35] The film thicknesses of the blends of both the polymers were similar (~70 nm), allowing for a good comparison of the PCEs (Table 2). The lower PCE of **P2** when compared with **P1** can be attributed to the different sizes of oxygen and sulfur atoms in the polymeric backbone of **P2** disrupting the packing of the polymer in the solid state. Both **P1** and **P2** display a lower PCE when compared with the benzodithiophene homopolymer **P3**.[34] This can be attributed to the lower solubility of both **P1** and **P2** in $CHCl_3$ when compared with **P3**.

Tapping-mode atomic force microscopic (TMAFM) analysis of both polymers **P1** and **P2** was performed on thin films obtained by drop-casting from $CHCl_3$ solutions on mica (Supporting Information). Both polymers **P1** and **P2** displayed a granular morphology (Supporting Information). To achieve further correlation between surface morphology and the solar cell performance, TMAFM analysis was performed on the solar cell devices of **P1** at 1:1 and 1:2 weight ratios (Fig. 3). The film obtained at polymer/PCBM 1:1 blend ratio had a uniform surface morphology, whereas the film obtained at 1:2 weight ratio had a more evident phase separation. The film obtained at 1:1 weight ratio is also smoother (RMS = 1.10 nm) than the film obtained at 1:2 weight ratio (RMS = 2.36 nm). This result is in agreement with our earlier observations that smoother blend films give higher PCEs in bulk heterojunction solar cells.[18,34] However, for polymer **P2**, the films obtained at both 1:1 and 1:2 weight ratios display similar surface roughness (RMS for 1:1 film = 2.54 nm, and RMS for 1:2 film = 2.83 nm). A comparison of the morphology of **P1** at 1:1 weight ratio (RMS = 1.10 nm) and **P2** at 1:1 weight ratio (RMS = 2.54 nm) further indicates that a smoother surface morphology yields higher performing solar cell devices (Fig. 4).

The field-effect mobilities of polymers **P1** and **P2** were measured in bottom-gate, bottom-contact organic field-effect transistors (OFETs). I_{DS}–V_{DS} curve families were recorded at different gate voltages [Fig. 5(a, c)]. The charge carrier mobility was determined by plotting $I_{DS}^{1/2}$ versus V_{GS} in the saturation regime [Fig. 5(b, d)], using the following equation:[22,36]

$$\mu = \frac{2L}{WC_i}\left[\frac{I_{DS}}{(V_{GS}-V_T)^2}\right],$$

where I_{DS} is the source-drain current, W is the channel width, L is the channel length, C_i is the capacitance of the silicon dioxide dielectric, V_{GS} is the gate voltage, and V_T is the threshold voltage. Polymers **P1** and **P2** had field-effect mobilities of 1.34×10^{-4} cm^2 V^{-1}s^{-1} and 3.00×10^{-5} cm^2 V^{-1}s^{-1}, which are higher than previously reported values for benzodifuran polymers.[37]

EXPERIMENTAL

Materials

All commercial chemicals were purchased from Aldrich Chemical and were used without further purification unless

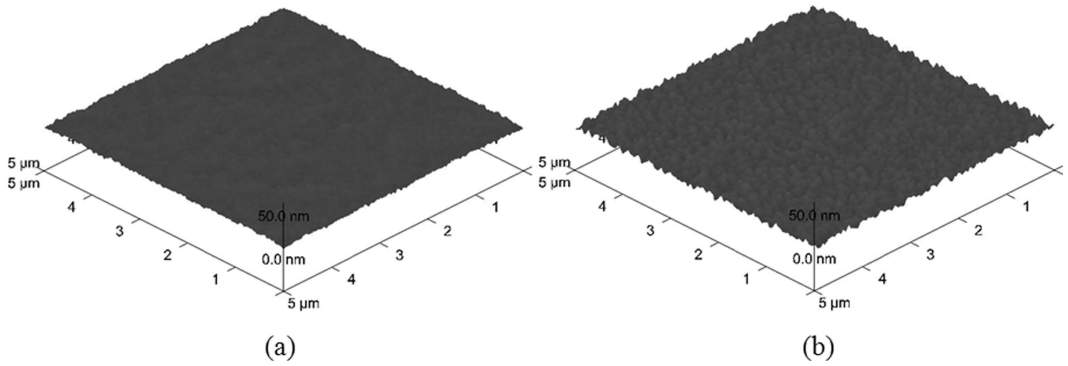

FIGURE 3 Three-dimensional TMAFM images of the active area of the solar cell devices of (a) [**P1**]:[PCBM] = 1:1 (RMS = 1.10 nm) and (b) [**P1**]:[PCBM] =1:2 (RMS = 2.36 nm).

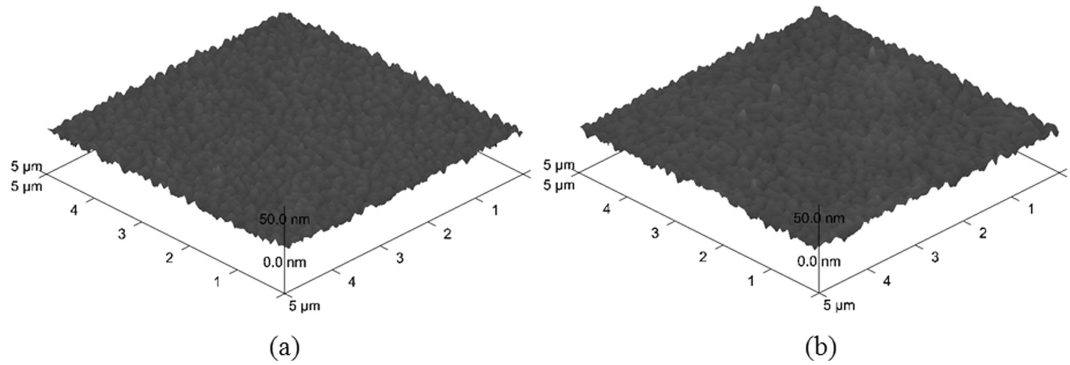

FIGURE 4 Three-dimensional TMAFM images of the active area of the solar cell devices of (a) [**P2**]:[PCBM] = 1:1 (RMS = 2.54 nm) and (b) [**P2**]:[PCBM] =1:2 (RMS = 2.83 nm).

otherwise noted. All reactions were conducted under purified nitrogen. The polymerization glassware and syringes were dried at 120 °C for at least 24 h before use and cooled under a nitrogen atmosphere. Tetrahydrofuran was dried over sodium/benzophenone ketyl and freshly distilled before use. 4,8-Dihydrobenzo[1,2-*b*:4,5-*b*′]dithiophene-4,8-dione was prepared according to a previously reported procedure.[38]

Structural Analysis

^{1}H NMR spectra of the synthesized monomers were recorded on a JEOL-Delta 270 MHz spectrometer at 25 °C. ^{1}H NMR spectra of the polymers were recorded on a VARIAN-INOVA-500 MHz spectrometer at 30 °C. ^{1}H NMR data are reported in parts per million as chemical shift relative to tetramethylsilane (TMS) as the internal standard. Spectra were recorded in $CDCl_3$. GC/MS was performed on an Agilent 6890-5973 GC-MS workstation. The GC column was a Hewlett-Packard fused silica capillary column crosslinked with 5% phenylmethyl siloxane. Helium was the carrier gas (1 mL min^{-1}). The following conditions were used for all GC/MS analyses: injector and detector temperature, 250 °C; initial temperature, 70 °C; temperature ramp, 10 °C min^{-1}; final

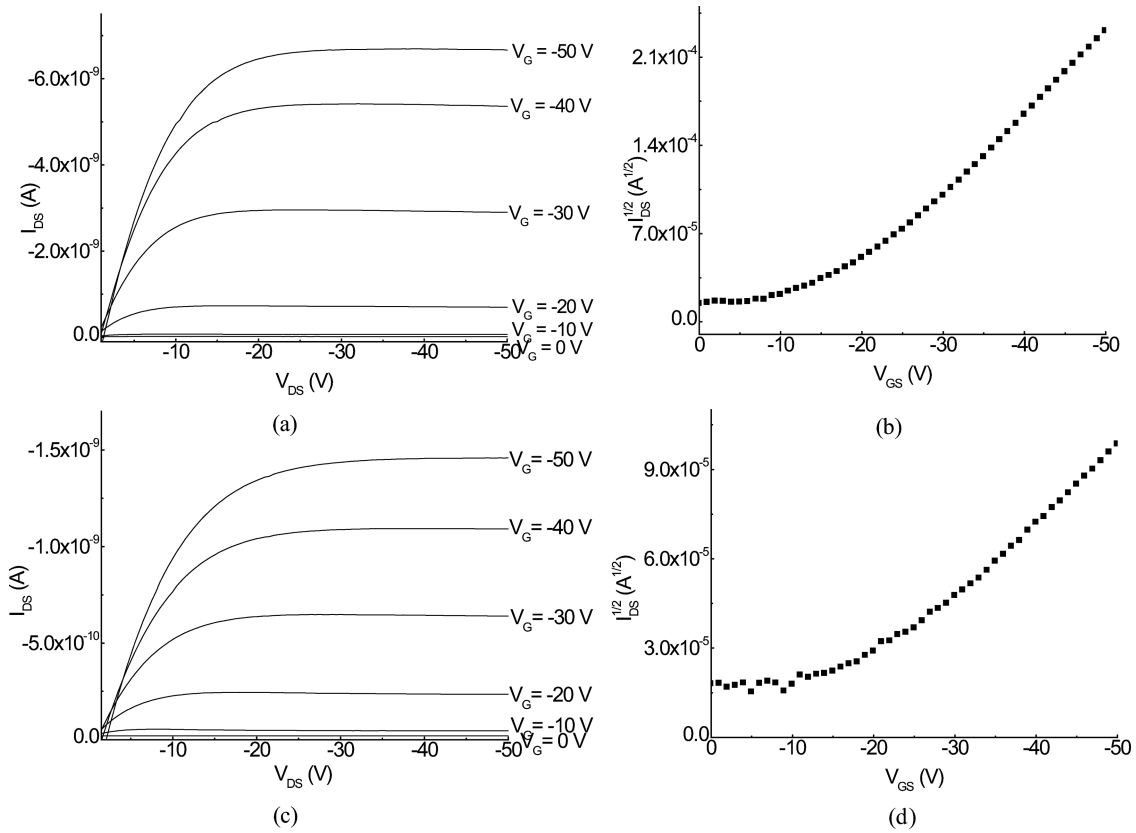

FIGURE 5 Current–voltage characteristics of polymers **P1** (a and b) and **P2** (c and d) for bottom-gate, bottom-contact OFETs: (a and c) output curves at different gate voltages and (b and d) transfer curves at $V_{DS} = -50$ V ($W = 475$ μm, $L = 20$ μm); polymer **P1**: $\mu = 1.34 \times 10^{-4}$ cm^2 V^{-1}s^{-1}, on/off ratio = 10^2, $V_T = -4.9$ V; polymer **P2**: $\mu = 3.00 \times 10^{-5}$ cm^2 V^{-1}s^{-1}, on/off ratio = 10^1, $V_T = -10.8$ V.

temperature, 280 °C. The UV–vis spectra of polymer solutions in chloroform solvent were carried out in 1-cm cuvettes using an Agilent 8453 UV–vis spectrometer. Thin films of polymer were obtained by evaporation of chloroform solvent on glass microscope slides. Molecular weights of the synthesized polymers were measured by size exclusion chromatography (SEC) analysis on a Viscotek VE 3580 system equipped with ViscoGEL™ columns (GMHHR-M), connected to a refractive index detectors. GPC solvent/sample module (GPCmax) was used with HPLC-grade THF as the eluent, and calibration was based on polystyrene standards. Running conditions for SEC analysis were as follows: flow rate = 1.0 mL min^{-1}; injector volume = 100 μL; detector temperature = 30 °C; column temperature = 35 °C. All the polymer samples were dissolved in THF, and the solutions were filtered through polytetrafluoroethylene (PTFE) filters (0.45 μm) prior to injection.

Tapping-Mode Atomic Force Microscopy

TMAFM investigation of thin-film surface morphology was carried out using a NanoscopeIV-Multimode Veeco, equipped with an E-type vertical engage scanner. Thin films were deposited by drop-casting chloroform solution of polymers on mica substrate. The AFM images were recorded at room temperature in air using silicon cantilevers with normal spring constant of 42 N m^{-1} and normal resonance frequency of 320 kHz. A typical value of AFM detector signal corresponding to RMS cantilever oscillation amplitude was equal to 1–2 V, and the images were collected at 0.5 Hz scan frequency in 2 μm scan size. Polymer samples were prepared in chloroform solutions (1 mg mL^{-1}) and deposited on mica substrate by drop-casting. TMAFM analysis was also performed on the solar cell devices.

Cyclic Voltammetry

Electrochemical grade tetrabutylammonium perchlorate (TBAP) was used as an electrolyte without further purification. Acetonitrile (99.9% grade) was distilled over calcium hydride. Electrochemical experiments were performed using a BAS CV-50W voltammetric analyzer. The electrochemical cell was composed of a platinum electrode, a platinum wire auxiliary electrode, and an Ag/AgCl reference electrode. Acetonitrile solutions containing 0.1 M of TBAP were placed in a cell and purged with argon. A drop of the polymer solution in chloroform was deposited on the tip of platinum electrode. The solvent was evaporated in air. The film was immersed in the electrochemical cell containing TBAP for measurement.

Synthesis of the Monomers

Synthesis of Furan-3-carbonyl chloride

Furan-3-carboxylic acid (10.00 g, 0.0893 mol) was heated at reflux with thionyl chloride (30 mL) in 100 mL of methylene chloride for 90 min. The solvent and the excess thionyl chloride were removed by distillation to yield a brownish solid. The solid was dissolved in 30 mL of methylene chloride and used for next step without purification.

Synthesis of N, N-Diethyl furan-3-carboxamide

Diethylamine (13.06 g, 0.179 mol) was diluted with 30 mL of methylene chloride and was added to a solution of furan-3-carbonyl chloride (0.0893 mol) in 30 mL of methylene chloride at 0 °C. The reaction mixture was stirred at room temperature for 2 h. The product was washed with water (2× 200 mL), dried with magnesium sulfate, filtered, and concentrated to yield brown oil, which was purified by vacuum distillation to yield 5.85 g of clear oil (0.035 mol, 39%).

^{1}H NMR ($CDCl_3$, 270 MHz) δ: 1.18 (t, 6H), 3.44 (q, 4H), 6.56 (d, 1H), 7.38 (d, 1H), 7.67 (s, 1H).

Synthesis of 4,8-Dihydrobenzo[1,2-b:4,5-b′] difuran-4,8-dione

N, N-Diethyl furan-3-carboxamide (5.85 g, 0.0350 mol) was diluted in 50 mL of dry THF. To this solution, 14.0 mL of 2.5 M *n*-BuLi in hexane (0.0350 mol) was added dropwise at 0 °C. The reaction mixture was warmed to room temperature and stirred at room temperature for 4 h. The reaction mixture was quenched with 300 mL of water and stirred overnight. The brownish solid was filtered to obtain 0.854 g of product (0.00454 mol, 26%).

^{1}H NMR ($CDCl_3$, 270 MHz) δ: 6.92 (d, 2H), 7.70 (d, 2H).

Synthesis of 4,8-Bis(4-decylphenylethynyl) benzo[1,2-b:4,5-b′]difuran

The synthesis of 4-decyl-1-ethynylbenzene was previously reported.[18] 4-Decyl-1-ethynylbenzene (2.13 g, 8.80 mmol) was dissolved in 50 mL of dry THF. At 0 °C, 3.5 mL of 2.5 M *n*-BuLi in hexane (8.80 mmol) was added to the solution of 4-decyl-1-ethynylbenzene dropwise under a nitrogen atmosphere. The reaction mixture was stirred for 5 min at 0 °C followed by the addition of 4,8-dihydrobenzo[1,2-*b*:4,5-*b*′]difuran-4,8-dione (0.820 g, 4.36 mmol) dissolved in 50 mL of THF. The reaction mixture was stirred for 30 min at reflux. The reaction mixture was cooled to room temperature followed by the addition of 4.42 g of tin chloride dihydrate dissolved in 60 mL of 20% HCl solution. The reaction mixture was refluxed for 30 min. The reaction mixture was diluted with ether (150 mL), and the organic layer was washed with water (2× 200 mL), dried with magnesium sulfate, filtered, and concentrated to yield a brownish solid, which was dissolved in 20 mL of THF and precipitated in 200 mL of methanol to yield an off-white solid. The solid was filtered to obtain 1.97 g of product (3.09 mmol, 71%).

^{1}H NMR ($CDCl_3$, 270 MHz) δ: 0.81 (t, 6H), 1.16 (m, 28H), 1.23 (m, 4H), 2.56 (t, 4H), 7.00 (d, 2H), 7.18 (d, 4H), 7.52 (d, 4H), 7.69 (d, 2H). ^{13}C NMR ($CDCl_3$, 270 MHz) δ: 14.21, 22.78, 29.36, 29.42, 29.59, 29.68, 31.34, 31.99, 36.07, 81.50, 98.60, 99.61, 106.99, 120.13, 127.55 128.64, 131.82, 144. 13, 146.27.

Synthesis of 2,6-Dibromo-4,8-bis(4-decylphenylethynyl)-benzo[1,2-b:4,5-b′]difuran

4,8-Bis(4-decylphenylethynyl)benzo[1,2-*b*:4,5-*b*′]difuran (0.905 g, 1.42 mmol) was dissolved in 100 mL of dry THF and cooled to −78 °C. To this solution, 1.20 mL of 2.5 M *n*-BuLi in hexane (3.0 mol, 2.1 equiv) was added, and the solution was stirred for 30 min at −78 °C. Carbon tetrabromide (1.007 g, 3.04 mmol, 2.14 equiv) dissolved in 20 mL of THF was added. After stirring for 5 min at −78 °C, the solution was allowed to warm to room temperature for 1 h. Solvent was removed, and

the brown solid was dissolved in chloroform and washed with water (2× 200 mL), dried with magnesium sulfate, and concentrated to obtain a brown solid. The brown solid was dissolved in 10 mL of THF and poured into 200 mL of methanol. The precipitated off-white solid was filtered to obtain 0.746 g of product (0.937 mmol, 60%).

^{1}H NMR ($CDCl_3$, 270 MHz) δ: 0.84 (t, 6H), 1.25 (m, 28H), 4.33 (m, 4H), 2.62 (t, 4H), 7.38 (s, 2H), 7.21 (d, 4H), 7.56 (d, 4H). ^{13}C NMR ($CDCl_3$, 100 MHz) δ: 14.21, 22.77, 29.41, 29.57, 29.67, 36.08, 36.19, 81.05, 98.41, 99.37, 108.88, 109.04, 119.75, 119.82, 128.22, 128.67, 129.30, 131.87, 144.31, 144.44, 151.87, 152.06.

Synthesis of 2,6-(Trimethyltin)-4,8-bis(4-decylphenylethynyl)-benzo[1,2-b:4,5-b′]difuran

4,8-Bis(4-decylphenylethynyl)benzo[1,2-*b*:4,5-*b*′]difuran (0.908 g, 1.42 mmol) was dissolved in 100 mL of dry THF. Under a nitrogen atmosphere at −78 °C, 1.20 mL of 2.5 M *n*-BuLi in hexane (3.0 mol, 2.1 equiv) was added. Reaction was stirred at −78 °C for 20 min followed by the addition of 3.0 mL of 1 M trimethyltin chloride. After the addition, the reaction was allowed to warm to room temperature for over 1 h. The solvent was evaporated, and the resultant solid was dissolved in chloroform, washed with water (2× 200 mL), dried with magnesium sulfate, filtered, and concentrated to yield a solid. The solid was dissolved in 10 mL of THF and added to 200 mL of methanol. The precipitated yellow solid was filtered to obtain 0.970 g of product (1.01 mmol, 71%).

^{1}H NMR ($CDCl_3$, 400 MHz) δ: 0.45 (s, 18H), 0.56 (t, 6H), 0.87 (m, 28H), 1.62 (m, 4H), 2.63 (t, 4H), 7.18 (d, 4H), 7.19 (s, 2H), 7.56 (d, 4H). ^{13}C NMR ($CDCl_3$, 270 MHz) δ: −8.78, 14.21, 22.77, 29.35, 29.42, 29.58, 29.69, 31.98, 36.06, 82.57, 97.81, 117.82, 120.65, 127.80, 128.58, 131.77, 143.76, 155.19, 167.47.

Synthesis of Poly{4,8-bis(4-decylphenylethynyl) benzo[1,2-b:4,5-b′]difuran}(P1)

To a three-necked round-bottomed flask, 2,6-dibromo-4,8-bis(4-decylphenylethynyl)benzo[1,2-*b*:4,5-*b*′]difuran (0.322 g, 0.405 mmol), 2,6-(trimethyltin)-4,8-bis(4-decylphenylethynyl)-benzo[1,2-*b*:4,5-*b*′]difuran (0.402 g, 0.417 mmol), and tetrakis(triphenylphosphine) palladium(0) (0.023 g, 0.0199 mmol) were added under a nitrogen atmosphere. Toluene (40 mL) and DMF (10 mL) were added to dissolve the monomers. The reaction mixture was heated at reflux for 72 h, and the polymer was precipitated in methanol. The polymer was filtered and was purified by Soxhlet extractions with methanol, diethyl ether, hexane, dichloromethane, and chloroform. The polymer was obtained from the chloroform fraction on evaporation of the solvent. The polymer was obtained as a dark red solid (0.360 g, 60% yield).

^{1}H NMR ($CDCl_3$, 500 MHz) δ: 0.88 (t, 6H), 1.25 (m, 12H), 1.52 (m, 20H), 2.62 (m, 4H), 6.9 (br, 8H), 7.6 (br, 2H).

Synthesis of Poly{4,8-bis(4-decylphenylethynyl)benzo[1,2-b:4,5-b′]difuran-alt-4,8-bis(4-decylphenylethynyl)-benzo[1,2-b:4,5-b′]dithiophene} (P2)

We have previously reported the synthesis and characterization of 2,6-(trimethyltin)-4,8-bis(4-decylphenylethynyl)-benzo [1,2-*b*:4,5-*b*′]dithiophene.[18]

To a three-necked round-bottomed flask, 2,6-(trimethyltin)-4,8-bis(4-decylphenylethynyl)-benzo[1,2-*b*:4,5-*b*′]dithiophene (0.314 g, 0.315 mmol), 2,6-dibromo-4,8-bis(4-decylphenylethynyl)benzo[1,2-*b*:4,5-*b*′]difuran (0.249 g, 0.313 mmol), and tetrakis(triphenylphosphine)palladium(0) (0.023 g, 0.020 mmol) were added under a nitrogen atmosphere. Toluene (40 mL) and DMF (8 mL) were added to dissolve the monomers. The solution was heated at reflux for 2 h, at which time 25 mL of toluene was added to the reaction mixture. After an additional 24 h at reflux, 0.020 g of the catalyst (0.017 mmol) was added to the reaction mixture, and after 48 h at reflux, an additional 0.025 g of catalyst was added. The polymerization was stopped after an additional 24 h at reflux by precipitating the polymer in methanol. The polymer was filtered, and the polymer was purified by Soxhlet extractions with methanol, diethyl ether, hexane, dichloromethane, and chloroform. The polymer was obtained from the chloroform fraction on evaporation of the solvent as a dark red solid (0.29 g, 70% yield).

^{1}H NMR ($CDCl_3$, 500 MHz) δ: 0.88 (m, 12H), 1.25 (m, 36H), 1.52 (m, 28H), 2.67 (m, 8H), 7.12–7.25 (br, 16H), 7.40 (br, 1H), 7.51 (br, 1H), 7.63 (br, 1H), 7.66 (br, 1H).

Solar Cells Fabrication and Testing

Organic light emitting diode (OLED)-grade glass slides coated with ITO were purchased from Luminescense Technology (Taiwan). The ITO on these slides was patterned using standard photolithography. The slides were cleaned with deionized water, acetone, and isopropanol successively by sonication for 20 min each and washed for 10 min in oxygen plasma before use. Immediately following plasma treatment, a 20 nm layer of PEDOT:PSS was spin coated onto the substrate (4000 min^{-1}, 1740 min^{-1} s^{-1}, 90 s), followed by annealing at 120 °C for 20 min under nitrogen. The PCBM/polymer blend was prepared in chloroform, at the required weight ratio of polymer and PCBM, with a constant total concentration of 15 mg mL^{-1}. This blend was then spin cast (2000 min^{-1}, 1740 min^{-1} s^{-1}, 60 s) onto the PEDOT-PSS/substrate. A cathode consisting of calcium (10 nm) was thermally evaporated at a rate of ∼1.0 Å s^{-1}, followed by aluminum (100 nm) at ∼2.5 Å s^{-1} through a shadow mask to define solar cell active areas.

IV testing was carried out under a controlled N_2 atmosphere using a Keithley 236, model 9160 power source interfaced with LabView software. The solar simulator used was a THERMOORIEL equipped with a 300-W xenon lamp; the intensity of the light was calibrated to 100 mW cm^{-2} with a NREL-certified Hamamatsu silicon photodiode. The active area of the devices was 0.09 cm^2.

Field-Effect Transistor (OFET) Fabrication and Mobility Determination

Field-effect mobility measurements of the synthesized polymers were performed on thin-film transistors with a common bottom-gate, bottom-contact configuration. Highly doped, *n*-type silicon wafers with a resistivity of 0.001–0.003 Ω cm were used as substrates. Silicon dioxide (SiO_2) (200 nm thickness) was thermally grown at 1000 C on the silicon

wafer. Chromium metal (5 nm) followed by 100 nm of gold was deposited by E-beam evaporation as source-drain metals. The source-drain pads were formed by photolithographically patterning the metal layer. The SiO_2 on the backside of the wafer was etched with buffered oxide etchant (7:1 BOE from JT Baker) to generate the common bottom gate. The resulting transistors had a channel width of 475 μm and channel length ranging from 2 to 80 μm. The measured capacitance density of the SiO_2 dielectric was 17 nF cm^{-2}. After the SiO_2 on the backside was removed, the devices were cleaned with UV–ozone for 7 min using a Technics Series 85 RIE etcher and stored under vacuum. This process removes any residual organics on the substrate. For the sample preparation of untreated devices, prior to the polymer deposition, the substrates were cleaned with water, methanol, hexanes, and chloroform with drying using N_2 flow between different solvents. The devices were baked at 80 °C for 30 min in a vacuum oven. The devices were allowed to cool under vacuum. For surface treatment with octyl trichlorosilane (OTS), the devices were rinsed sequentially with water, methanol, hexanes, and chloroform and placed in a glass container in a solution of OTS of 4×10^{-3} M in dried toluene. The sealed container was placed in a glove box at ambient temperature for 48 h. After 48 h, the device was taken out of the glove box and rinsed with toluene before baking it at 80 °C for 30 min in a vacuum oven. The polymer films were deposited in air by drop-casting 4–5 drops of 1 mg mL^{-1} polymer solution prepared in HPLC-grade chloroform and filtered through a 0.2-μm PTFE filter using a 25-μL syringe. The devices were allowed to dry in a Petri dish saturated with chloroform. The devices were annealed under vacuum for 30 min at 120 °C prior to measurements. The devices were again allowed to cool down to room temperature under vacuum. A Keithley 4200-SCS semiconductor characterization system was used to probe the devices. The probe station used for electrical characterization was a Cascade Microtech Model Summit Microchamber. When measuring current–voltage curves and transfer curves, V_G was scanned from −50 V to +5 V. All the measurements were performed at room temperature in air.

CONCLUSIONS

We have synthesized a new benzodifuran monomer 4,8-bis (4-decylphenylethynyl)benzo[1,2-*b*:4,5-*b*′]difuran and polymerized it by Stille coupling polymerization to obtain poly{4,8-bis(4-decylphenylethynyl)benzo[1,2-*b*:4,5-*b*′]difuran} homopolymer (**P1**). An alternating copolymer poly{4,8-bis(4-decylphenylethynyl)benzo[1,2-*b*:4,5-*b*′]difuran-*alt*-4,8-bis(4-decylphenylethynyl)benzo [1,2-*b*:4,5-*b*′]dithiophene} (**P2**) was also synthesized. The polymers yielded reasonable molecular weights: 29,600 g mol^{-1} for **P1** and 22500 g mol^{-1} for **P2**. The HOMO energy levels of these polymers were between −5.39 and −5.30 eV, and the LUMO energy were between −3.32 and −3.26 eV. Bulk heterojunction solar cell measurements on both the polymers revealed that **P1** displayed a maximum PCE of 1.19% at 1:1 weight ratio of polymer and PCBM, whereas **P2** displayed a maximum PCE 0.79% at 1:2 weight ratio. The lower PCE of **P2** when compared with **P1** can be attributed to the different sizes of oxygen and sulfur atoms in the polymeric backbone of **P2** disrupting the packing of the polymer in its solid state. TMAFM analysis of the polymers was performed for films of pristine polymer deposited on mica and for blends used as active layer in the solar cell devices. A granular morphology was observed for both polymers **P1** and **P2**. The TMAFM analysis of the polymer/PCBM blends indicated that films with smoother surface morphology displayed higher power conversion efficiencies.

ACKNOWLEDGMENTS

Mihaela C. Stefan acknowledges the financial support from the NSF (DMR-0956116) and the Welch Foundation (AT-1740). The authors thank Dr. Anvar Zakhidov at UT Dallas for giving access to the solar cell measurement setup.

REFERENCES AND NOTES

1 Handbook of Conducting Polymers; Skotheim, T. A.; Reynolds, J., Eds.; CRC Press: Boca Raton, **2006.**

2 Handbook of Thiophene-Based Materials: Applications in Organic Electronics and Photonics; Perepichka, I. F.; Perepichka, D. F., Eds.; Wiley: West Sussex, **2009**.

3 Ma, W.; Yang, C.; Gong, X.; Lee, K.; Heeger, A. J. *Adv. Funct. Mater.* **2005,** *15*, 1617–1622.

4 Reyes-Reyes, M.; Kim, K.; Dewald, J.; Lopez-Sandoval, R.; Avadhanula, A.; Curran, S.; Carroll, D. L. *Org. Lett.* **2005,** *7*, 5749–5752.

5 Sauve, G.; Javier, A. E.; Zhang, R.; Liu, J.; Sydlik, S. A.; Kowalewski, T.; McCullough, R. D. *J. Mater. Chem.* **2010,** *20*, 3195–3201.

6 Beaujuge, P. M.; Subbiah, J.; Choudhury, K. R.; Ellinger, S.; McCarley, T. D.; So, F.; Reynolds, J. R. *Chem. Mater.* **2010,** *22*, 2093–2106.

7 Hou, J.; Chen, H.-Y.; Zhang, S.; Chen, R. I.; Yang, Y.; Wu, Y.; Li, G. *J. Am. Chem. Soc.* **2009,** *131*, 15586–15587.

8 Hou, J.; Chen, H.-Y.; Zhang, S.; Li, G.; Yang, Y. *J. Am. Chem. Soc.* **2008,** *130*, 16144–16145.

9 Hou, J.; Park, M.-H.; Zhang, S.; Yao, Y.; Chen, L.-M.; Li, J.-H.; Yang, Y. *Macromolecules* **2008,** *41*, 6012–6018.

10 Huo, L.; Hou, J.; Zhang, S.; Chen, H.-Y.; Yang, Y. *Angew. Chem. Int. Ed. Engl.* **2010,** *49*, 1500–1503.

11 Liang, Y.; Wu, Y.; Feng, D.; Tsai, S.-T.; Son, H.-J.; Li, G.; Yu, L. *J. Am. Chem. Soc.* **2009,** *131*, 56–57.

12 Liang, Y.; Yu, L. *Acc. Chem. Res.* **2010,** *43*, 1227–1236.

13 Pan, H.; Li, Y.; Wu, Y.; Liu, P.; Ong, B. S.; Zhu, S.; Xu, G. *Chem. Mater.* **2006,** *18*, 3237–3241.

14 Pan, H.; Li, Y.; Wu, Y.; Liu, P.; Ong, B. S.; Zhu, S.; Xu, G. *J. Am. Chem. Soc.* **2007,** *129*, 4112–4113.

15 Piliego, C.; Holcombe, T. W.; Douglas, J. D.; Woo, C. H.; Beaujuge, P. M.; Frechet, J. M. J. *J. Am. Chem. Soc.* **2010,** *132*, 7595–7597.

16 Price, S. C.; Stuart, A. C.; Yang, L.; Zhou, H.; You, W. *J. Am. Chem. Soc.* **2011,** *133*, 4625–4631.

17 Sista, P.; Biewer, M. C.; Stefan, M. C. *Macromol. Rapid Commun.* **2012,** *33*, 9–20.

18 Sista, P.; Nguyen, H.; Murphy, J. W.; Hao, J.; Dei, D. K.; Palaniappan, K.; Servello, J.; Kularatne, R. S.; Gnade, B. E.; Xue, B.; Dastoor, P. C.; Biewer, M. C.; Stefan, M. C. *Macromolecules* **2010,** *43*, 8063–8070.

19 Wang, Y.; Parkin, S. R.; Watson, M. D. *Org. Lett.* **2008,** *10*, 4421–4424.

20 Zou, Y.; Najari, A.; Berrouard, P.; Beaupre, S.; Reda Aich, B.; Tao, Y.; Leclerc, M. *J. Am. Chem. Soc.* **2010,** *132*, 5330–5331.

21 Beaujuge, P. M.; Frechet, J. M. J. *J. Am. Chem. Soc.* **2011,** *133*, 20009–20029.

22 Sista, P.; Bhatt, M. P.; McCary, A. R.; Nguyen, H.; Hao, J.; Biewer, M. C.; Stefan, M. C. *J. Polym. Sci. Part A: Polym. Chem.* **2011,** *49*, 2292–2302.

23 Shiraishi, K.; Yamamoto, T. *Synth. Met.* **2002,** *130*, 139–147.

24 Leenen, M. A. M.; Cucinotta, F.; Pisula, W.; Steiger, J.; Anselmann, R.; Thiem, H.; De Cola, L. *Polymer* **2010,** *51*, 3099–3107.

25 He, Z.; Zhong, C.; Huang, X.; Wong, W.-Y.; Wu, H.; Chen, L.; Su, S.; Cao, Y. *Adv. Mater.* **2011,** *23*, 4636–4643.

26 Yiu, A. T.; Beaujuge, P. M.; Lee, O. P.; Woo, C. H.; Toney, M. F.; Frechet, J. M. J. *J. Am. Chem. Soc.* **2012,** *134*, 2180–2185.

27 Gidron, O.; Dadvand, A.; Sheynin, Y.; Bendikov, M.; Perepichka, D. F. *Chem. Commun.* **2011,** 1976–1978.

28 Huo, L.; Huang, Y.; Fan, B.; Guo, X.; Jing, Y.; Zhang, M.; Li, Y.; Hou, J. *Chem. Commun.* **2012,** 3318–3320.

29 Bunz, U. H. F. *Angew. Chem. Int. Ed. Engl.* **2010,** *49*, 5037–5040.

30 Li, H.; Jiang, P.; Yi, C.; Li, C.; Liu, S.-X.; Tan, S.; Zhao, B.; Braun, J. R.; Meier, W.; Wandlowski, T.; Decurtins, S. *Macromolecules* **2010,** *43*, 8058–8062.

31 Chu, Q.; Pang, Y. *Spectrochim. Acta Part A* **2004,** *60*, 1459–1467.

32 Birckner, E.; Grummt, U. W.; Goeller, A. H.; Pautzsch, T.; Egbe, D. A. M.; Al-Higari, M.; Klemm, E. *J. Phys. Chem. A* **2001,** *105*, 10307–10315.

33 Brown, P. J.; Thomas, D. S.; Kohler, A.; Wilson, J. S.; Kim, J.-S.; Ramsdale, C. M.; Sirringhaus, H.; Friend, R. H. *Phys. Rev. B: Condens. Matter Mater. Phys.* **2003,** *67*, 064203/1–064203/16.

34 Sista, P.; Xue, B.; Wilson, M.; Holmes, N.; Kularatne, R. S.; Nguyen, H.; Dastoor, P. C.; Belcher, W.; Poole, K.; Janesko, B. G.; Biewer, M. C.; Stefan, M. C. *Macromolecules* **2012,** *45*, 772–780.

35 Scharber, M. C.; Mühlbacher, D.; Koppe, M.; Denk, P.; Waldauf, C.; Heeger, A. J.; Brabec, C. J. *Adv. Mater.* **2006,** *18*, 789–794.

36 Bhatt, M. P.; Huynh, M. K.; Sista, P.; Nguyen, H. Q.; Stefan, M. C. *J. Polym. Sci. Part A: Polym. Chem.* **2012,** *50*, 3086–3094.

37 Li, H.; Tang, P.; Zhao, Y.; Liu, S.-X.; Aeschi, Y.; Deng, L.; Braun, J.; Zhao, B.; Liu, Y.; Tan, S.; Meier, W.; Decurtins, S. *J. Polym. Sci. Part A: Polym. Chem.* **2012,** *50*, 2935–2943.

38 Beimling, P.; Kobmehl, G. *Chem. Ber.* **1986,** *119*, 3198–3203.